Research Article

Mediterranean Marine Science
Indexed in WoS (Web of Science, ISI Thomson) and SCOPUS
www.hcmr.gr
DOI: https://doi.org/10.12681/mms.40883

Genetic structure and connectivity of the critically endangered deep-sea octocoral *Isidella elongata*: implications for marine biodiversity conservation in the Mediterranean Sea

Valentina LAURIA[1,2,3], Francesco GARGANO[4,3], Marco ARCULEO[2], Gioacchino BONO[1,2,3], Fabio FIORENTINO[1,5], Jean-François FLOT[6,7], Olivier COLLARD[6], Maria Cristina FOLLESA[8], Germana GAROFALO[1,3] Vincent GEORGES[1], Porzia MAIORANO[9], Daniela MASSI[1,3,10], Caterina STAMOULI [11], Sandrine VAZ[12], Sergio VITALE[1,3], and Luca VECCHIONI[2]

[1] The Institute for Marine Biological Resources and Biotechnology of the National Research Council, Mazara del Vallo, Italy
[2] Department of Biological, Chemical and Pharmaceutical Sciences and Technologies, University of Palermo, Palermo, Italy
[3] National Biodiversity Future Center, Palermo, Italy
[4] Department of Engineering, University of Palermo, Palermo, Italy
[5] Stazione Zoologica Anton Dohrn, Palermo, Italy
[6] Evolutionary Biology & Ecology, Université libre de Bruxelles, Brussels, Belgium
[7] Interuniversity Institute of Bioinformatics in Brussels - (IB)², Brussels, Belgium
[8] Department of Life Science and Environment, University of Cagliari, Italy
[9] Department of Biosciences, Biotechnologies and Environment, University of Bari Aldo Moro, Bari, Italy
[10] Italian Institute for Environmental Protection and Research, Palermo, Italy
[11] Institute of Marine Biological Resources & Inland Waters, Hellenic Centre for Marine Research, Athens, Greece
[12] MARBEC, Univ Montpellier, CNRS, Sète, Ifremer, IRD, France

Corresponding author: Valentina LAURIA; valentina.lauria@cnr.it

Contributing Editor: Costas TSIGENOPOULOS

Received: 21 March 2025; Accepted: 11 September 2025; Published online: 17 December 2025

Abstract

The protection of the Vulnerable Marine Ecosystem identified by the presence of the critically endangered bamboo coral *Isidella elongata* has been recognized as an urgent task. Although some research has focused on the spatial distribution of this species, there is no information available on its connectivity and genetic structure. This is the first study to examine the genetic diversity pattern and inter-population connectivity of *I. elongata* at the Mediterranean scale. The DNA-based approach for assessing the genetic diversity of 33 *I. elongata* samples collected in six different areas involved two mitochondrial markers (COI and MutS) and one nuclear marker (ITS2). Molecular results confirmed that all samples belonged to *I. elongata* and showed a scarce level of intra- and inter-population mtDNA differentiation, whereas nuDNA data revealed genetic structuring. Furthermore, a Lagrangian model (forward-in-time simulations) was used to investigate the species larval connectivity under different sea current conditions. Our results suggest the presence of persistent pathways, supporting the self-sustaining nature of the populations, especially in the central Mediterranean Sea. This study identifies the main corridors of connectivity for *I. elongata* in the Mediterranean Sea, highlighting the importance of including such information in the implementation of fishery management measures.

Keywords: Connectivity; Deep water corals; Larval dispersal; Mediterranean Sea; Molecular analysis.

Introduction

The Mediterranean Sea, with its biodiversity and ecological complexity, has long been recognized as a biodiversity hotspot: some 17,000 species account for 7.5% of the species richness of oceans (Coll *et al.*, 2010; Danovaro & Pusceddu, 2007; Lejeusne *et al.*, 2010). Among these species, deep-sea coral assemblages play an important role in benthic ecosystems, providing essential three-dimensional habitats for marine communities and representing biodiversity hotspots (Bongiorni *et al.*, 2010; Carbonara *et al.*, 2022). Mediterranean deep-sea coral habitats are characterised by a relatively dense aggregation of scleractinian colonies *of Desmophyllum pertusum* (Linnaeus, 1758), *Madrepora oculata* (Linnaeus, 1758) and *Desmophyllum dianthus* (Esper, 1794) as well as by soft, compact mud facies characterized by the sea pen *Funiculina quandrangularis* (Pallas, 1766) and the gorgonian *Isidella elongata* (Esper, 1788) (Chimienti *et al.*, 2019). In many places, these important habitats are

found to overlap with the fishing grounds for commercially valuable crustaceans; they are therefore targeted by bottom trawling fisheries (i.e., soft bottom coral gardens; Fabri *et al.*, 2014; Lauria *et al.*, 2017; Georges *et al.*, 2024), which represent a threat to their conservation.

Habitats that include Octocorallia, Antipatharia and Scleractinia (habitat-forming species) have been classified as Vulnerable Marine Ecosystems (VMEs) (United Nations Resolution A/RES/61/105) since 2006. To protect these sensitive deep-sea habitats, Fisheries Restricted Areas (FRAs) have been implemented by the General Fisheries Commission for the Mediterranean Sea (GFCM) as a multi-purpose spatial-management tool to restrict fishing activities (https://www.fao.org/gfcm/data/maps/fras/fr/). However, these measures are limited either to certain depths (currently below 1000m across the whole Mediterranean Sea, despite the suggestion to move this limit to 800 m depth) or to specific areas, which leaves many VMEs unprotected. The identification of priority areas for conservation of VMEs at the Mediterranean scale also meets the required restoration and protection of impacted areas by 2050 under the Nature Restoration Law (2024).

At present, several studies have investigated the spatial distribution of some VME indicator species to prioritize areas for biodiversity conservation in the Mediterranean Sea under fisheries and climate change impacts (Fabri *et al.*, 2014; Lauria *et al.*, 2017; Gerovasileiou *et al.*, 2019; Carbonara *et al.*, 2020; González-Irusta *et al.*, 2022; Wang *et al.*, 2022; Georges *et al.*, 2024; Millot *et al.*, 2024). These studies have investigated the effects of environmental conditions on habitat selection, as well as the ecological role of these species, but have neglected other crucial aspects such as population structure and connectivity. The importance of acquiring information on species genetic variability and connectivity patterns has been largely discussed among scientists, and the Kunming-Montreal Global Biodiversity Framework has highlighted the urgency of prioritizing genetic diversity to safeguard the adaptive potential of populations (CBD/COP/15/L25, 2022). In addition, the Group on Earth Observations Biodiversity Observation Network (GEO BON) has proposed the "genetic composition Essential Biodiversity Variables" (genetic EBVs) as standardized metrics for tracking within-species genetic variation and informing policy. These data can help designate key areas and associated corridors that need to be protected, with the final aim of informing fisheries policy and supporting marine spatial planning.

One of the most at-risk indicator species of Vulnerable Marine Ecosystems (VMEs) in the Mediterranean Sea is the bamboo coral *Isidella elongata*. This branching deep-sea octocoral is generally found at depths over 200m and is closely associated with a bathyal mud biocoenosis (*sensu* Peres & Picard, 1964; Chimienti *et al.*, 2020). This species is quasi-endemic in the Mediterranean Sea, having also been detected at moderately high densities in the Gulf of Cádiz (Rueda *et al.*, 2019). The three-dimensional structure of *I. elongata* provides shelter from predators to fish and crustacean species (Mastrototaro *et al.*, 2017), which can also find a high density of prey within its canopy (Maynou & Cartes, 2012).

The species is not only a habitat-former but also provides a secondary hard biological substratum for other species such as epibionts and a spawning substratum for cephalopods and sharks (Laubier & Emig, 1993). Consequently, *I. elongata* grounds have been shown to positively influence marine biodiversity (Buhl-Mortensen *et al.*, 2010; Maynou & Cartes, 2012; Mytilineou *et al.*, 2014; Mastrototaro *et al.*, 2017; Carbonara *et al.*, 2022). Nevertheless, because of its life-history traits and its co-occurrence with bottom-trawling target species such as deep-sea shrimps *Aristeus antennatus* (Risso, 1816) and *Aristaeomorpha foliacea* (Risso, 1827) (Lauria *et al.*, 2017; Mastrototaro *et al.*, 2017; Cartes *et al.*, 2022), this species is listed as "Critically Endangered" in the IUCN Red List: its abundance has declined by over 80% in the last four decades (Otero *et al.*, 2017). By contrast, some healthy assemblages of this species have been found at shallower depths in areas of the northwest Mediterranean Sea where fishing activities are prohibited (Angiolillo *et al.*, 2024). As human-induced processes such as climate change and deep-water fishing continue to have a significant negative impact on marine habitats at a quickening pace, understanding the genetic structure and connectivity patterns of *I. elongata* could improve the design of effective conservation and management strategies.

Molecular techniques have improved the ability to study potential patterns of connectivity among marine populations (Hellberg *et al.*, 2002). Genetic connectivity, considered as the exchange of individuals between populations, is a crucial determinant of a species' resilience to environmental changes and of its ability to persist over time (White *et al.*, 2010). In the marine environment, connectivity is assessed from genetic diversity structure or parentage analysis using molecular biology techniques (Mackenzie *et al.*, 2022). In addition, demographic connectivity (the exchange of individuals and genes between populations) can be studied from larval dispersal patterns derived from oceanic circulation simulations (Pineda *et al.*, 2007). Aside from molecular techniques, Lagrangian transport models were coupled with large-scale oceanographic models that it possible to investigate the dispersal of early life stages (eggs/larvae). In these models, eggs and larvae are represented as passive particles transported by current fields derived from numerical ocean models. Lagrangian models have been applied to a wide range of species, including pelagic and demersal fish (Gargano *et al.*, 2017, 2022; Quattrocchi *et al.*, 2019; Torri *et al.*, 2023), sedentary benthic invertebrates, and corals such as the red coral *Corallium rubrum* (Linnaeus, 1758) and the bubblegum coral *Paragorgia arborea* (Linnaeus, 1758) (Guizien & Bramanti, 2014; Wang *et al.*, 2022). These models allow the identification of spatiotemporal patterns of larval dispersal connecting spawning areas to settlement areas, which in turn help to identify key areas to be proposed for conservation.

The present study explored the genetic diversity and inter-population connectivity of *Isidella elongata* in the Mediterranean Sea using a framework based on both molecular techniques and larval dispersal modelling. These two combined approaches allowed the identification of

corridors of deep-sea coral connectivity, supporting future conservation measures such as a network of Fisheries Restricted Areas. First, a molecular approach was used to assess the genetic diversity of the sampled bamboo coral specimens collected in six different areas spread across the Mediterranean Sea (from the Gulf of Lion to the Aegean Sea); this involved the characterization of two mitochondrial (mtDNA) markers, i.e., a fragment of the cytochrome *c* oxidase subunit I (COI) and a portion of the mitochondrial genome comprising part of the *nad4L* gene and of the *mutS* gene (MutS), as well as of a nuclear (nuDNA) marker, the internal transcribed spacer 2 (ITS2) located in ribosomal DNA. The use of COI as a universal species-level barcode for animals was proposed over a decade ago (Hebert *et al.*, 2003), even though its resolution is lower in cnidarians and sponges than in bilaterian animals (Shearer *et al.*, 2002; Huang *et al.*, 2008). MutS is instead a marker specific to octocorals (Pont-Kingdon *et al.*, 1995) that offers species-level resolution, although this mtDNA marker has limited discriminatory power in some taxa and does not consistently resolve species boundaries in octocorals (Calderon *et al.*, 2006; Gori *et al.*, 2012; Aurelle *et al.*, 2017). Conversely, ITS2 has been repeatedly used as a marker of choice to delimit species of hexacorals (Flot & Tillier, 2006; Terrana *et al.*, 2021) and octocorals (e.g., Korfhage *et al.*, 2022). It coalesces faster than other nuclear markers because of its concerted mode of evolution (Liao, 1999), making it easier to use it to delineate species, but recently diverged species may still exhibit incomplete lineage sorting for this marker (see Aurelle *et al.*, 2011), in which case methods that do not not rely on monophyly, such as haplowebs (Flot *et al.*, 2010), are required to delineate species properly.

A Lagrangian model (forward-in-time simulations) was then used to model and predict potential *I. elongata* larval spatial connectivity patterns in the Mediterranean Sea. The results of this study can inform conservation strategies aimed at preserving deep-sea coral species and their associated biodiversity within the Mediterranean Sea. Moreover, the combination of these two approaches (modelling and genetics) can help clarify the processes that influence the genetic structuring and dispersion of deep-water corals.

Materials and Methods

Sample collection

Isidella elongata samples were collected from 2017 to 2022 at 33 sites in six areas of the Mediterranean Sea (Table 1, Fig. 1). Most of the samples were obtained from the Mediterranean International Trawl Survey (MEDITS) programme, an annual bottom trawling survey conducted across various regions of the Mediterranean Sea since 1994; the surveys, realized in late spring to early summer, adopt a standardised sampling methodology (MEDITS, 2017). All samples were frozen on board and morphologically identified at the species level in the laboratory. Taxonomic identification of *I. elongata* was carried out according to Carpine & Grasshoff (1975) and Rossi (1971). The species has a whitish colour and presents a typical candelabra-like morphology, with numerous branches and non-retractile polyps. The skeleton presents a clear alternation of white carbonate internodes and brown protein nodes similar to joints, from which the branches

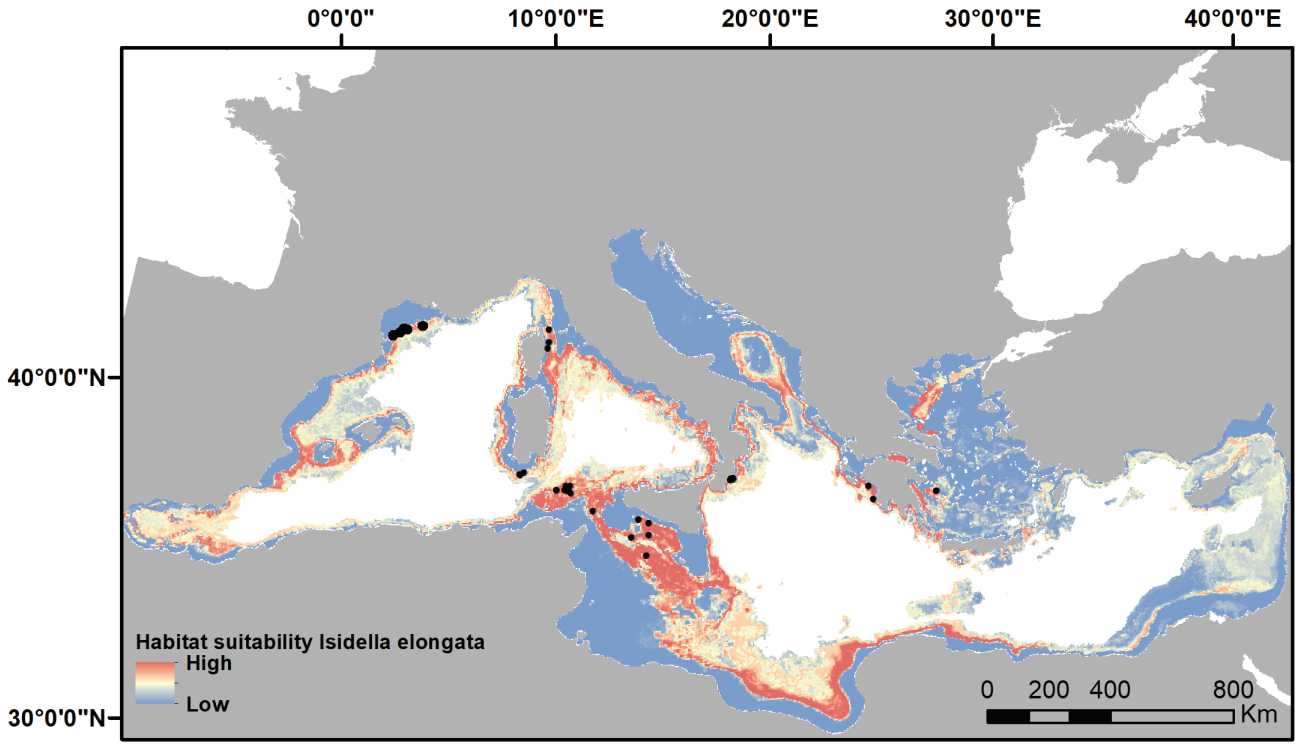

Fig. 1: Geographic location of the sampling sites. Black circles indicate sites where *Isidella elongata* was sampled. The habitat suitability of the species in the Mediterranean Sea is also shown (from Georges *et al.*, 2024).

Table 1. Summary of *Isidella elongata* samples used in the present study. Information about the survey during which samples were collected and the targeted area, as well as sampling coordinates expressed as decimal degrees and depth are provided. GenBank accession numbers are also indicated.

Code	GenBank accession numbers			Survey	Year	Area	Latitude	Longitude	Depth (m)	Source
	COI	MutS	ITS2							
VME004	PX274210	PX283514	PX275455-PX275456	MEDITS	2021	Strait of Sicily	37.0815	13.3268	314.50	Institute for Marine Biological Resources and Biotechnology
VME005	PX274210	PX283515	PX275457	MEDITS	2021	Strait of Sicily	36.6696	12.6957	619	Institute for Marine Biological Resources and Biotechnology
VME006	PX274210	PX283516	PX275458	MEDITS	2021	Strait of Sicily	36.1214	13.1932	659.5	Institute for Marine Biological Resources and Biotechnology
VME007	PX274210	PX283517	PX275459	MEDITS	2021	Strait of Sicily	36.7244	13.3211	656.50	Institute for Marine Biological Resources and Biotechnology
VME008	PX274210	PX283518	PX275460-PX275461	MEDITS	2021	Strait of Sicily	37.1897	12.9700	314.50	Institute for Marine Biological Resources and Biotechnology
VME017	PX274210	PX283519	PX275462-PX275463	MEDITS	2022	Corsica	42.8420	9.7149	522	Jadaud & Certain, 2022
VME018	PX274210	PX283520	PX275464-PX275465-PX275466	MEDITS	2022	Corsica	42.3087	9.6822	413.50	Jadaud & Certain, 2022
VME019	PX274210	PX283521	PX275467-PX275468	MEDITS	2022	Corsica	42.4836	9.7252	534	Jadaud & Certain, 2022
VME020	PX274210	PX283522	PX275469	MEDITS	2022	Gulf of Lion	42.6803	4.1118	420	Jadaud & Certain, 2022
VME021	PX274210	PX283523	PX275470-PX275471	MEDITS	2022	Gulf of Lion	42.6931	3.9549	802.50	Jadaud & Certain, 2022
VME022	PX274210	PX283524	PX275472-PX275473	MEDITS	2022	Gulf of Lion	42.5775	3.8401	680	Jadaud & Certain, 2022
VME023	PX274210	PX283525	PX275474-PX275475	MEDITS	2022	Gulf of Lion	42.8194	4.6955	664.50	Jadaud & Certain, 2022

Continued

Table 1 continued

Code	GenBank accession numbers			Survey	Year	Area	Latitude	Longitude	Depth (m)	Source
	COI	MutS	ITS2							
VME025	PX274210	PX283526	PX275476	MEDITS	2022	Sardinia Channel	38.5675	8.6556	N.A.	University of Cagliari
VME026	PX274210	PX283527	PX275477	MEDITS	2022	Sardinia Channel	38.5636	8.6898	N.A.	University of Cagliari
VME027	PX274210	PX283528	PX275478-PX275479	MEDITS	2022	Sardinia Channel	38.6368	8.8121	N.A.	University of Cagliari
VME028	PX274210	PX283529	PX275480	MEDITS	2022	Ionian Sea	21.3666	37.5262	622	Hellenic Centre for Marine Research
VME029	PX274210	PX283530	PX275481-PX275482	MEDITS	2022	Ionian Sea	21.4535	37.1147	744	Hellenic Centre for Marine Research
VME030	PX274210	PX283531	PX275483	MEDITS	2022	Aegean Sea	23.7353	37.0487	698	Hellenic Centre for Marine Research
VME031	PX274210	PX283532	PX275484-PX275485	MEDITS	2022	Aegean Sea	23.7353	37.0487	698	Hellenic Centre for Marine Research
VME059	PX274210	PX283533	PX275486	MAYNOU 2	2022	Egadi Islands	38.2500	10.5200	576	Institute for Marine Biological Resources and Biotechnology
VME060	PX274210	PX283534	PX275487	MAYNOU 2	2022	Egadi Islands	38.1300	10.0100	709.20	Institute for Marine Biological Resources and Biotechnology
VME061	PX274210	PX283535	N.A.	MAYNOU 2	2022	Egadi Islands	38.1300	10.3500	601.20	Institute for Marine Biological Resources and Biotechnology
VME062	PX274210	PX283536	PX275488	MAYNOU 2	2022	Egadi Islands	38.1000	10.4300	559.80	Institute for Marine Biological Resources and Biotechnology
VME063	PX274210	PX283537	PX275489-PX275490	MAYNOU 2	2022	Egadi Islands	38.100	9.4200	620	Institute for Marine Biological Resources and Biotechnology

Continued

Table 1 continued

Code	GenBank accession numbers			Survey	Year	Area	Latitude	Longitude	Depth (m)	Source
	COI	MutS	ITS2							
VME064	PX274210	PX283538	PX275491-PX275492	MAYNOU 2	2022	Egadi Islands	38.1300	10.3490	599	Institute for Marine Biological Resources and Biotechnology
VME067	PX274210	PX283539	PX275493	MAYNOU 2	2022	Egadi Islands	38.0400	10.5490	604	Institute for Marine Biological Resources and Biotechnology
VME070	PX274210	PX283540	N.A.	MEDITS	2017	Calabria	38.2023	16.3937	558.00	University of Bari
VME071	PX274210	PX283541	N.A.	MEDITS	2017	Calabria	38.2023	16.3937	558.00	University of Bari
VME072	PX274210	PX283542	PX275494-PX275495	MEDITS	2018	Calabria	38.233	16.4322	553.00	University of Bari
VME073	PX274210	PX283543	PX275496-PX275497	MEDITS	2021	Calabria	38.2090	16.5180	713.50	University of Bari
VME074	PX274210	PX283544	PX275498-PX275499	MEDITS	2018	Calabria	38.2356	16.4370	547.50	University of Bari
VME075	PX274210	PX283545	PX275500	MEDITS	2020	Calabria	38.2353	16.4335	515.50	University of Bari
VME076	PX274210	PX283546	PX275501-PX275503	MEDITS	2018	Calabria	38.2361	16.4377	549.50	University of Bari
VME077	PX274210	N.A.	PX275504-PX275505	MEDITS	2018	Calabria	38.2330	16.4322	553.00	University of Bari
VME078	PX274210	PX283547	PX275506-PX275507	MEDITS	2022	Sardinia Channel	38.5675	8.6556	N.A.	University of Cagliari
VME079	PX274210	PX283548	PX275508-PX275509	MEDITS	2022	Sardinia Channel	38.5636	8.6898	N.A.	University of Cagliari
VME080	PX274210	PX283549	PX275510	MEDITS	2022	Sardinia Channel	38.6368	8.8121	N.A.	University of Cagliari

originate (Bayer & Stefani, 1987), as well as a root-like structure that anchors the colony in the compact mud. After species identification, a fragment of coral tissue was collected from each sample and kept in 96% ethanol for DNA extraction.

DNA extraction and sequencing

Coral tissue from the polyps was ground prior to DNA extraction using the BIORON GmbH "Ron's Tissue DNA Mini Kit". Fragments of the mtDNA markers COI and MutS and the complete nuDNA Internal Transcribed Spacer 2 (ITS2) were amplified through Polymerase Chain Reaction (PCR). The primer pair "LCO1490" and "HCO2198" (Folmer *et al.*, 1994) was used to amplify COI, whereas the primer pair "Co3Bam5657f" (Brugler & France, 2008) and "MUT3458R" (Sánchez *et al.*, 2003) was used to amplify the MutS marker; the ITS2 nuDNA marker was amplified using the primer pair "ITSc2-5" and "R28S1" described by Flot *et al.* (2008).

The COI fragment was amplified in a 25-µl volume containing 1.5 µl of genomic DNA, 2.5 µl of Buffer 10X (including 15 mM of $MgCl_2$), 0.3 µl of dNTPs (10 mM of each), 0.3 µl of forward and reverse primers (10 µM), 0.35 µl of BIORON DFS-Taq DNA Polymerase 5U/µL, and 19.75 µl of double-distilled water. After an initial 5 min denaturation phase at 96 °C, the PCR consisted of 35 cycles with denaturation (1 min at 95 °C), annealing (1 min at 48 °C) and extension (1 min at 72 °C), plus a final extension cycle of 8 min at 72 °C. The MutS PCR mix and thermal cycles consisted of 1 µL of genomic DNA, 2.5 µL buffer 10X including 15 mM $MgCl_2$ solution, 0.5 µL dNTPs (10 mM of each), 0.5 µL of forward and reverse primers (10 µM), 0.3 µL BIORON DFS-Taq DNA Polymerase 5U/µL, and 19.7 µL double-distilled water, for a total volume of 25 µL. The thermal cycle consisted of a 2 min denaturation step at 94 °C, followed by 35 cycles with denaturation (1 min at 94 ºC), annealing (1 min at 56.5 ºC) and extension (1.30 min at 72 ºC), followed by a final 5 min extension step at 72 ºC. Lastly, the ITS2 nuDNA fragment was amplified in 25-µL volume including 1.5 µL of genomic DNA, 2.5 µL buffer 10X (with 15 mM $MgCl_2$), 0.5 µL dNTPs (10 mM of each), 0.5 µL of both forward and reverse primers (10 µM), 0.3 µL BIORON DFS-Taq DNA Polymerase 5U/µL, and 19.2 µL of double-distilled water. The thermal cycle consisted of initial denaturation at 94 °C for 1 min, followed by 40 cycles with denaturation at 94°C for 30 sec, annealing at 53 °C for 30 sec, and extension at 72 °C for 1.15 min, and then a final 7 min extension at 72 °C.

PCR products were separated using 1% agarose gel electrophoresis and visualized through a UV transilluminator. Only samples that displayed a unique clear band of the expected length for the marker used were purified using the Exo-SAP-IT® kit (Affymetrix USB) and subsequently sequenced with an ABI 3130xL sequencer by Macrogen Inc. (Madrid, Spain). The primers used for the PCRs were also used for the sequencing of PCR products. In addition, as some of the ITS2 Sanger sequences showed poor quality due to contamination by other organisms (notably *Funicularia*), we resequenced these individuals (as well as a few additional ones) using the LSK114 Nanopore kit on a Flongle flow cell to facilitate the cleaning and deconvolution of the mixed traces of heterozygous individuals. COI and MutS chromatograms were checked and edited using MEGA11 (Tamura *et al.*, 2021) and aligned using the Clustal W method (Thompson *et al.*, 1994), as implemented in the software MEGA11. ITS2 forward and reverse sequences were assembled together as suggested by Fontaneto *et al.* (2015), using Sequencer v4.1.4 (Gene Codes). Haplotypes were reconstructed from mixed Sanger sequencing traces using Champuu (Flot & Tillier, 2006; Flot, 2007; Spöri & Flot, 2024) and SeqPHASE (Flot, 2010; Spöri & Flot, 2024) and were aligned using Mafft's E-INS-i mode (Katoh *et al.*, 2019). All novel *Isidella elongata* sequences were deposited in GenBank (accession numbers PX274210 for COI, PX283514-PX283549 for MutS and PX275455-PX275510 for ITS2).

To compare the new MutS sequences with those publicly available, 39 *Isidella* spp. sequences were downloaded from GenBank and included in the analyses (see Fig. 3A for their accession numbers). All sequences were aligned using the MAFFT web server (available at http://mafft.cbrc.jp/alignment/server/large.html; Katoh *et al.*, 2019). Moreover, the software MEGA11 (Tamura *et al.*, 2021) was used to identify possible misalignments by visual inspection. Lastly, to detect any sequencing errors or the occurrence of pseudogenes, all MutS sequences were translated into amino acids, allowing the identification of frameshifts and stop codons.

Bayesian inference (BI) of phylogeny, as implemented in the software package MrBayes v. 3.2.7 (Ronquist *et al.*, 2012), and maximum likelihood (ML) analyses, using PhyML v. 3.0 (Guindon *et al.*, 2010), were performed on the mtDNA MutS dataset to investigate phylogenetic relationships among the analysed sequences. The best evolutionary model was selected from among those analysed by MrBayes using Bayesian model choice criteria (nst = mixed, rates = invgamma). Two independent MCMC analyses were conducted with 1,000,000 generations each. Trees and parameter values were sampled every 1,000 generations, discarding the initial 25% of trees as burn-in, resulting in 10,000 trees for each analysis. Convergence of chains was assessed to ensure proper mixing, reaching an ESS (Effective Sample Size) > 200 in all the performed analyses. Bootstrap values were calculated with 1,000 replicates in the ML trees, whereas posterior probability (PP) values were reported for the BI trees.

Haplotype networks, including all the novel *I. elongata* sequences, were built for the mtDNA MutS and the nuDNA ITS2 datasets using the Median-Joining method (Bandelt *et al.*, 1999) implemented in the HaplowebMaker online tool (Spöri & Flot, 2020) available at https://eeg-ebe.github.io/HaplowebMaker/.

The Lagrangian model

A Lagrangian forward-in-time simulation model was used to study the dispersal of *Isidella elongata* larvae from the sampled locations (Fig. 1). This approach assumes that eggs and larvae act as passive particles transported by sea currents. Their movement is determined by a three-dimensional marine velocity field, which includes data from both large-scale and small-scale simulations to account for turbulence in marine currents. The main large-scale marine current velocity fields were extracted from the Mediterranean Sea physical reanalysis (MEDREA) system (available at https://doi.org/10.48670/mds-00375). This dataset, referred to as U_{MFS}, comprises daily averaged northward and eastward velocity components of marine currents in the Mediterranean Sea with a horizontal grid resolution of 1/24° (approximately 4-5 km) in 141 unevenly spaced vertical levels. In addition, two artificial time-dependent, smaller-scale velocity fields named U_{2D} and U_{3D} were incorporated to capture the nearly chaotic complexity of marine currents. The U2D field, a bidimensional velocity field, was used to replicate both i) unresolved sub-mesoscale processes or sub-grid-scale variations that were poorly resolved at the resolution of the MEDREA reanalysis, given that these features are often associated with dynamics occurring at or below the scale of the Rossby radius in the Mediterranean (~10 km, Grilli & Pinardi, 1998): and ii) the super-diffusive Richardson regime (see Lacorata *et al.*, 2008, 2014). The U_{3D} field is a three-dimensional velocity field designed to simulate turbulent vertical mixing by introducing 3D vortical structures that can extend to 40 meters in depth. These fields were designed to enhance the model's accuracy in representing the dynamic, complex nature of marine currents at these critical scales (Fig. 2). The model has been successfully applied to analyse the connectivity patterns of various species in the central Mediterranean Sea, both in the forward-in-time context (Gargano *et al.*, 2017; Palatella *et al.*, 2014; Quattrocchi *et al.*, 2019) and in the backward-in-time context (Gargano *et al.*, 2022); full model details are reported in the Appendix.

The model setup is essentially based on information available on the species. Previous research has suggested that deep Mediterranean gorgonian species have a single reproductive season during summer, similarly to shallow species (Chimienti *et al.*, 2019). Our scenario analyses were therefore performed using daily averaged currents during June and July. Although the duration of the pelagic larval period is unknown for *I. elongata*, Hilário *et al.* (2015) report a range of between 7 and 90 days for alcyonacean corals and gorgonians, whereas other studies consider an average of 60 days (L. Bramanti, *personal communication*; Metaxas *et al.*, 2019). The *Isidella elongata* larvae show low dispersal ability (Otero *et al.*, 2017). Two dispersal components have been observed in other coral species: a passive component defined by the larvae (in general negative, leading to sinking) and an active component determined by larval swimming activity (Martínez-Quintana *et al.*, 2015; Mulla *et al.*, 2020).

In view of this, particles were released daily during June and July and tracked forward in time for 60 days. From 2016 to 2020, a total of 3,960 Lagrangian particles (1,980 pairs following the quasi-Lagrangian approach, see the Appendix for details) were released daily throughout June and July. The designated release areas coincide with regions where the species is known to be present

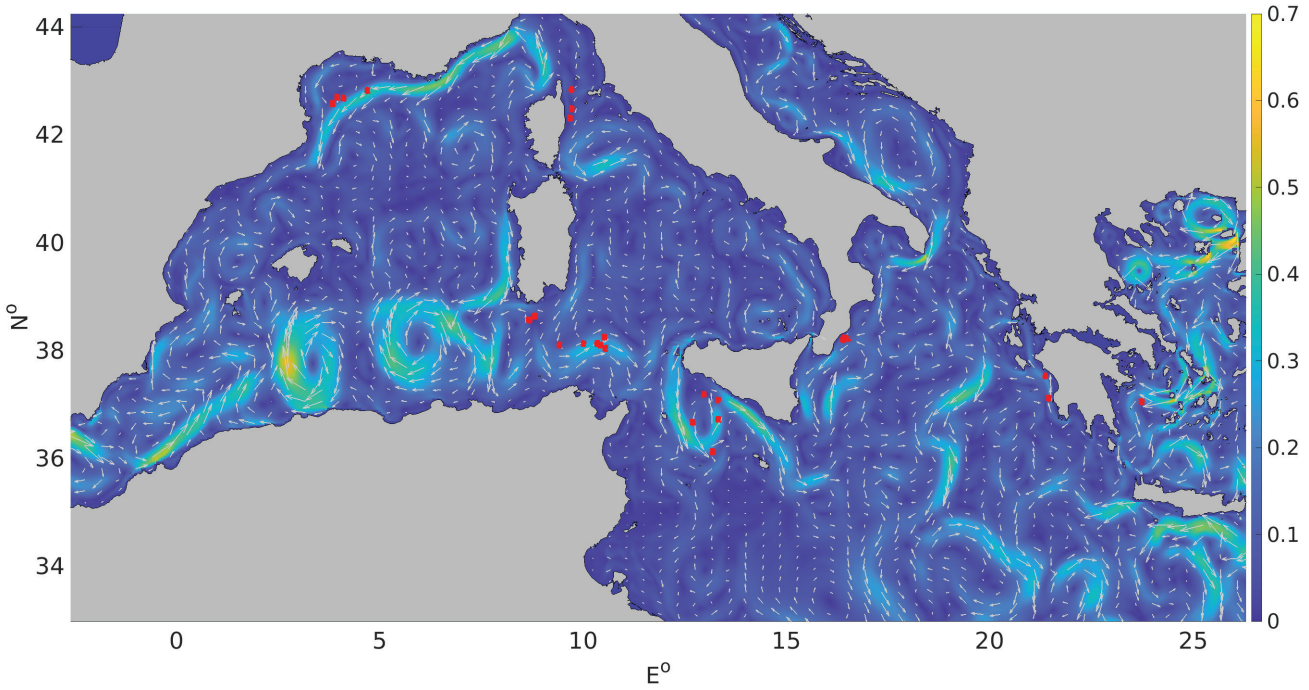

Fig. 2: Large-scale oceanographic circulation in the Mediterranean Sea; the monthly mean for July 2018 is shown as an example because some patterns and values are relatively stable over time. The colour scale indicates the intensity of the currents expressed as velocity (meters/second), with blue indicating low velocity and yellow high velocity. Red circles indicate points where *Isidella elongata* was sampled (release points in the Lagrangian simulations).

(Fig. 1). Notably, 60 pairs were randomly positioned within 33 squares, each spanning 0.05˚ x 0.05˚, centred on the locations indicated in Table 1. As information on the larval behaviour of *Isidella elongata* is scarce, two distinct scenarios were explored to account for potential unknown factors influencing larval dispersal. In the first scenario, S_{unif}, particles were randomly placed throughout the water column, whereas in the second, S_{sup}, they were released at the water surface. The first scenario is based on the understanding that vertical mixing and weak-moderate buoyancy effects could rapidly distribute the released eggs across the water column, and simulations are set to begin after this distribution time. This assumption is particularly relevant in the upper layers, where mixing is more effective. The second scenario aims to examine the potential for significant dispersal processes, assuming that larvae exhibit strong active swimming capabilities or buoyancy that significantly affect the vertical mixing process (assuming it is enhanced by swimming and hindered by buoyancy due to lipid content). These scenarios were selected to account for various vertical behaviours that have not yet been studied in this species, providing a deeper understanding of the dispersal process.

Hotspot identification and correlation index

Potential arrival areas for *Isidella elongata* larvae were identified and mapped through hotspot analysis. The Mediterranean region was divided into 1/8 ° × 1/8 ° (14 km x 14 km) cells, larger than the resolved cells of the UMFS, excluding the inland cells. For each year, particle counts were performed within each cell every 6 hours during the final ten days of their dispersal, resulting in 40 sampling times per particle. The abundance index of each cell was subsequently calculated for each year by simply summing all the particle counts for each individual cell. The Getis-Ord gi* analysis (Getis & Ord, 1992) was applied to identify the arrival hotspots of *I. elongata* Ω based on the analysis of the z-score (or p-level) values for each cell, calculated by averaging the eight neighbouring cells. Following Gargano *et al.* (2017), for each year, cells with a z-score above a threshold value (zthr = 4) were identified as hotspots. This threshold was selected after several trials to overcome the zero-inflated nature of the data, as many cells had few or no particles. This approach aims to highlight true abundance, avoiding the identification of an excessive number of hotspots with only a few particles. In the various trials (not shown here), relatively small changes in the threshold (in the range 2–6) did not alter qualitative outcomes: the abundance index retained its peak in the same areas, and the hotspot region around the peaks only slightly decreased or increased whenever the threshold value was lowered or raised. After identifying hotspot cells for each year, we calculated the number of years in which each cell was marked as a hotspot relative to the total number of years. This ratio, ranging from 0 to 1, is referred to as a persistence index (PI) and reflects how consistently a cell is classified as a hotspot over time. In our analysis, we established a Correlation Index (CI) to link the initial spawning areas with significant hotspots, namely regions where the PI was at least 0.5. The CI was calculated using a methodology similar to the one adopted by Huret *et al.* (2007) and Gargano *et al.* (2022). In particular, for a generic particle i initially released in the year j in spawning region s, the correlation index with the nursery n, $CI_{i,j}^{s,n}$, is defined as the portion of time (values in the range [0,1]) that a particle spends over the selected arrival area in the last 10 days of its dispersal (we checked for the position of a particle every six hours to obtain a more refined result with 60 samples). The global $CL^{s,n}$ for the s-th spawning area and n-th settlement areas in the period 2016-2020 was then computed as the mean value of the various $CI_{i,j}^{s,n}$ over the years and the number of particles:

$$CI^{s,n} = \left(\sum_{j=2016}^{2020} \frac{\sum_i CI_{i,j}^{s,n}}{N_j} \right) / 5$$

where N_j is the total number of particles released in the year j. This value, always in the range [0,1], can be considered a measure of the contribution of each release area to recruitment in the various arrival areas.

Results

DNA extraction, amplification and sequencing

Overall, 37 specimens were identified as *Isidella elongata* using morphological criteria (Table 1). The mitochondrial COI and MutS markers were successfully amplified in 37 and 36 individuals, respectively; ITS2 sequences were produced for a subset of 34 individuals only, since some of the obtained chromatograms were heavily contaminated and were therefore discarded (see Table 1 for further information). Results of the mtDNA COI and MutS translation into amino acids did not reveal stop codons and showed an amino acid sequence shared across the sequences. The COI sequences obtained (with a length of 636 bp) showed no variation among the analysed samples, leading us to exclude this mitochondrial gene from the analyses, and to provide the only haplotype found as a reference sequence (GenBank accession number PX274210). For the other mtDNA marker used in the present study (i.e., the MutS homologue), the inferred BI and ML phylogenetic trees, based on an 819 base-pair long fragment including both novel and published sequences, were rooted on *Mopseidae* sp. (GenBank accession number ON109717). Both phylogenetic trees showed a congruent clustering of the analysed sequences with a well-supported topology. Nevertheless, our novel sequences all clustered within the same clade, indicating low intraspecific variation (uncorrected *p*-distance of 0.05%).

The haplotype network based on the mtDNA fragment revealed four haplotypes, of which three were exclusive and one was shared among different geographic areas, with the only exception of the Aegean samples. All the remaining haplotypes detected were connected to the

main common haplotype by one to three mutational steps (Fig. 3B).

The *Isidella elongata* haplotype network based on the nuclear ITS2 marker (593-bp long) shows five haplotypes, of which three were shared among populations and two were exclusive. The fact that all haplotypes were connected by heterozygous individuals in the haploweb (Fig. 3C) confirms that they all belong to a single species or "field for recombination" (FFR) following the criterion of mutual allelic exclusivity (Doyle *et al.*, 1995; Flot *et al.*, 2010).

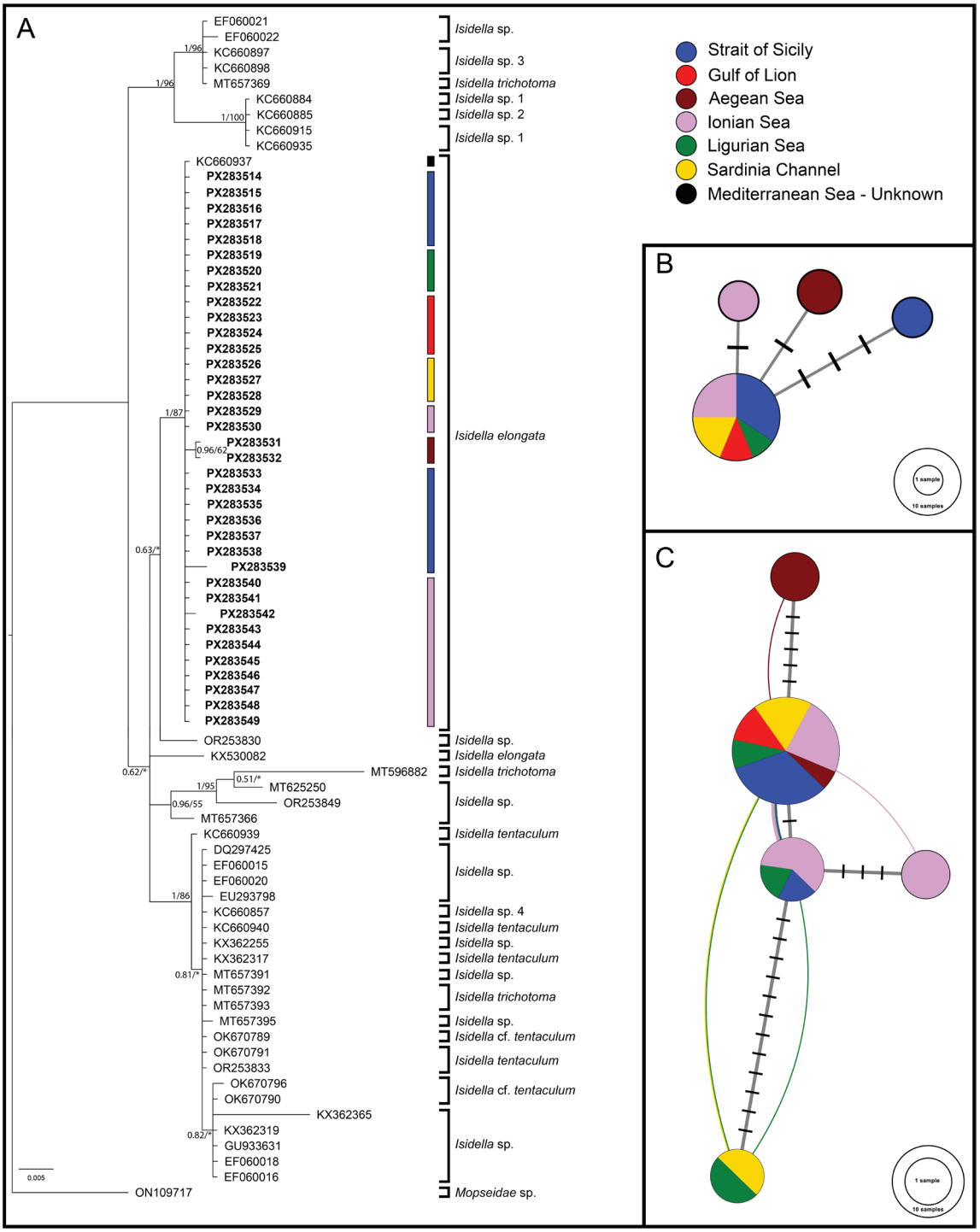

Fig. 3: A) Bayesian phylogram of *Isidella* spp. sequences based on the 819-bp long mtDNA MutS fragment. A sequence of *Mopseidae* sp. (A.N., ON109717) was used as outgroup. Node statistical support is reported as nodal posterior probabilities (Bayesian Inference of phylogeny, BI) and bootstrap values (Maximum Likelihood, ML). Novel mtDNA MutS *Isidella elongata* sequences are reported in bold. B) Median-joining haplotype network based on the novel mtDNA MutS *Isidella elongata* sequences. Dashes indicate substitution steps. Each circle represents a haplotype, and its size is proportional to its frequency. Colours refer to those reported in Figure 3A. C) Median joining haplotype network based on the novel 593-bp long nuDNA ITS2 *Isidella elongata* sequences. Dashes indicate substitutions steps. Haplotypes found co-occurring in heterozygous individuals are connected by Bézier curves, the thickness of which represents the frequency of these heterozygotes. Each circle represents a haplotype, and its size is proportional to its frequency. Colours are as in Figure 3A.

Regional-scale connectivity patterns

The results of Persistent Index analysis for both scenarios (S_{unif} and S_{sup}) and connectivity patterns (Tables 2 and 3) are shown in Figure 4. In the S_{unif} scenario, significant arrival areas having a PI of at least 0.5 were predominantly located near the release areas, indicating a possible high level of local retention. This result was also supported by the calculated CI index (Table 2), which in some cases indicated moderate-high values between proximate release and arrival areas. For example, release area R1 (Gulf of Lion) had a CI value of 0.24, with arrival area A11 also located nearby (Fig. 4A). The R2 release area (Corsica) was highly correlated (CI=0.47) with arrival area A12 (Corsica), and the two areas overlaped almost entirely. By contrast, release area R3 (Sardinia Channel) showed a more intricate CI structure. The highest CI (0.3426) was associated with arrival area A7, which included the area around the spawning sites in the Sardinia Channel. A lower CI of 0.0091 also indicates connectivity with A9, the smaller arrival area near the southwestern coast of Sardinia.

Our results showed weaker connections (CI of order 10^{-4}), with arrival areas A1 and A3, located in the Strait of Sicily (Table 2; Fig. 4A). There was minimal but observable connectivity (CI of the order 10^{-6}) with arrival area A12 in Corsica. Release area R4 (Strait of Sicily) primarily connected to arrival area A3 near the Sicilian coast (CI=0.1647). A weaker connection was also observed with arrival area A1, which is closer to the African coast (CI=0.0246; Fig. 4A), and with the large A5 arrival area situated in the western Ionian Sea, off the coast of Sicily (CI=0.0003). In the Ionian Sea, release area R5 showed the strongest connectivity with arrival area A5 (western Ionian Sea), located close to the release area (CI=0.3731), and to a lesser extent with arrival area A8 (CI=0.0028), which could actually be considered a part of A5 (Fig. 4A). Lastly, release areas R6 (eastern Ionian Sea) and R7 (Aegean Sea) were predominantly connected to arrival areas A6 and A4, respectively, almost overlapping with the release sites: R6 had a CI=0.3836 with A6, and R7 had a CI=0.6632 with A4 (Table 2; Fig. 4A).

In the S_{sup} scenario, the stronger surface currents lead to enhanced dispersal, with some similarities in the arrival areas like in the previous scenario; however, CI values were much lower than in the S_{unif} scenario (Table 3; Fig. 4B), with a reduced number of hot spots. There were some differences; for example a new arrival area, A1, was identified near the Tunisian coast (the Gulf of Gabés), whereas arrival areas A1 and A3 (in the Strait of Sicily) of the S_{unif} scenario no longer appeared. Release area R1 (Gulf of Lion) showed moderate connectivity with arrival areas A5 and A6 (Balearic Sea), which are part of the larger structure near the Spanish coast, and had a CI of 0.106 and 0.043, respectively. Release area R2 (Corsica) predominantly connected with arrival area A7 (Ligurian Sea), exhibiting a moderate CI=0.114. There was also weak but noticeable connectivity (CI= 0.009) with arrival area A3 (Sardinia Channel). Release area R3 (Sardinia Channel) displayed a weak to moderate correlation with nearby arrival areas A3 andA4 (CIs of the order of 10^{-2}). Release area R4 (Strait of Sicily) had a connection with arrival area A1 only (Gulf of Gabés), showing a weak CI= 0.016. Release area R5 (western Ionian Sea) had a moderate connection with arrival area A2, with CI=0.130. Lastly, release areas R6 and R7 (eastern Ionian Sea and Aegean Sea) did not correlate with any arrival areas (Fig. 4B).

Table 2. Correlation Index (CI) for the Sunif scenario between release areas (R1-R7) and arrival areas (A1-A12) shown in Figure 4A. The higher values (>0.10) of the CI representing the correlation between release and arrival areas are shaded in grey. Arrival areas A2 and A10 are not indicated in the figure as these show no correlation

Release/ Arrival areas	A1 Strait of Sicily	A2	A3 Strait of Sicily	A4 Aegean Sea	A5 Western Ionian Sea	A6 Eastern Ionian Sea	A7 Sardinia Channel	A8 Western Ionian Sea	A9 Sardinia Channel	A10	A11 Gulf of Lion	A12 Corsica
R1 Gulf of Lion	0	0	0	0	0	0	0	0	0	0	0.2440	0
R2 Corsica	0	0	0	0	0	0	0.0013	0	0	0	0	0.4706
R3 Sardinia Channel	0.0003	0	0.0005	0	0	0	0.3426	0	0.0091	0	0	$6 \cdot 10^{-6}$
R4 Strait of Sicily	0.0246	0	0.1647	0	0.0003	0	0	0.0000	0	0	0	0
R5 Western Ionian Sea	0	0	0	0	0.3731	0	0	0.0028	0	0	0	0
R6 Eastern Ionian Sea	0	0	0	0	0	0.3886	0	0	0	0	0	0
R7 Aegean Sea	0	0	0	0.6632	0	0	0	0	0	0	0	0

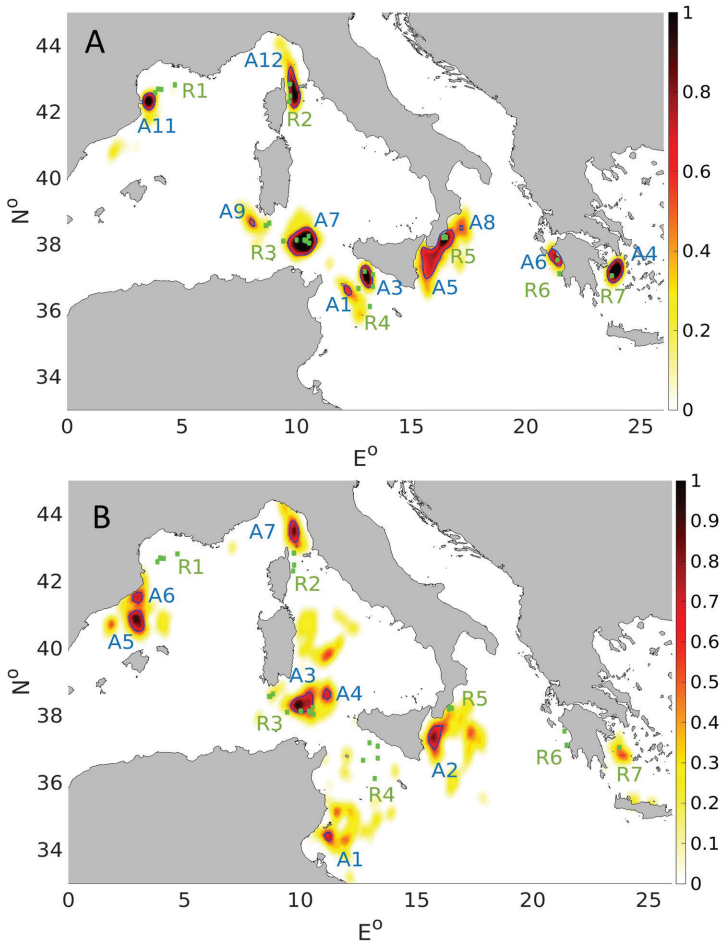

Fig. 4: Arrival areas A1-A12 (areas for which hotspot analysis yielded a persistence index of at least 0.5 in both scenarios) are shown and outlined by the dark-blue contour lines. The uniform release scenario output is shown in the top map (A), and the surface release scenario output is shown in the bottom map (B). In panel (A), areas A2 and A10 are not shown as they have zero connectivity in that scenario. As the velocity of the currents is different in the water column, the output of the surface release scenario (B) indicates a wider dispersion of the *Isidella elongata* larvae than in the uniform scenario (A). Grouped release sites are marked with green dots labelled R1-R7.

Table 3. Correlation index (CI) for the Ssup scenario between release areas (R1-R7) and arrival areas (A1-A12) shown in Figure 4B. The higher values (>0.10) of the CI representing the correlation between release and arrival areas are shaded in grey.

Release/Arrival areas	A1 Gulf of Gabés	A2 Western Ionian Sea	A3 Sardinia Channel	A4 Sardinia Channel	A5 Balearic Sea	A6 Balearic Sea	A7 Ligurian Sea
R1 Gulf of Lion	0	0	0	0	0.106	0.043	0
R2 Corsica	0	0	0.009	0.000	0	0	0.114
R3 Sardinia Channel	0	0	0.073	0.011	0	0	0
R4 Strait of Sicily	0.016	0.000	0	0	0	0	0
R5 Western Ionian Sea	0	0.130	0	0	0	0	0
R6 Eastern Ionian Sea	0	0	0	0	0	0	0
R7 Aegean Sea	0	0	0	0	0	0	0

Discussion

This study provides new insight into connectivity patterns and the genetic structure of populations of the critically endangered deep-water coral *Isidella elongata* at the Mediterranean scale. The combination of molecular analysis and Lagrangian particle tracking modelling is a framework that can be applied to similar studies and can be used to inform fisheries management plans while ensuring biodiversity conservation through the designation of areas for protection of VMEs.

Our morphological and molecular results confirm that all the investigated Mediterranean coral populations belong to *Isidella elongata* (Fig. 3). However, the phylogenetic position of one of the two publicly available *I. elongata* sequences (KX530082) raises concerns that the specimen used to produce it may have been misidentified (as suggested by Saucier, 2016). Conversely, the other available *I. elongata MutS* sequence (i.e., KC660937) clustered together with our novel MutS sequences, suggesting the soundness of our data. The nuDNA ITS2 results (Fig. 3C) show a higher genetic structuring with all of the detected haplotypes were connected by heterozygous individuals, implying that some individuals of the studied populations may have had or still have a connection with other distant Mediterranean populations. Similar studies have investigated the genetic structure of the deep-sea scleractinian *Desmophyllum pertusum* across the Mediterranean Sea and the northeast Atlantic through the use of specific microsatellite markers and ribosomal internal transcribed spacer (ITS) markers ITS1 and ITS2; results indicate genetic structuring of *D. pertusum* in the sampled locations, which was greater among fjord populations than open sea populations. Geographical distance did not correlate with genetic differentiation among the subpopulations distributed along the European margin (Le Goff-Vitry *et al.*, 2004). Other studies have evidenced strong genetic differentiation among populations of other octocorals (*Paramuricea clavata*) at different spatial scales (from local to basin scale) and across depths (at local scale) (Mokhtar-Jamai *et al.*, 2011). Such high genetic structuring was also observed at the regional scale for both *Corallium rubrum* and *P. clavata* in the northwestern Mediterranean Sea, suggesting that similar mechanisms such as hydrodynamic and oceanographic barriers (e.g., presence of fronts) may influence the well-defined structure of these species (Mokhtar-Jamai *et al.*, 2011; Ledoux *et al.*, 2010a). Another important factor driving gene differentiation among populations of octocorals (e.g., *P. clavata* and *C. rubrum*) is distance, most probably because of the short larval dispersal distance of many species (Mokhtar-Jamai *et al.*, 2011; Ledoux *et al.*, 2010a; Ledoux *et al.*, 2010b). Similarly, our results for *I. elongata* reveal a marked genetic structure: for some areas, this is probably linked to the distance between sites where the samples were collected.

The results of the Lagrangian model for both scenarios suggest the presence of persistent pathways, supporting the self-sustaining nature of the populations, especially in the central Mediterranean Sea. For example, in both scenarios, outputs suggest that the Sardinia Channel is a highly suitable habitat for *Isidella elongata* and is a larval arrival hotspot; although to a lesser extent, this result was also found for the western Ionian Sea and the Aegean Sea (Fig. 1; 4). Lagrangian model results suggest that areas with suitable habitats (Fig. 1) represent corridors of connectivity between slope populations and other deep-slope populations benefitting from passive larval dispersal.

There are some differences between the two scenarios: the output of the S_{unif} scenario clearly identifies hotspots for the arrival of *Isidella el*ongata larvae (Fig. 4A), whereas these are less evident in the S_{sup} scenario (Fig. 4B). This is likely to depend on the different scenario settings, particularly the depth at which the larvae meet the current that transports them; this suggests that vertical larval behaviour has a role in the connectivity pattern of this species. The S_{unif} scenario exhibits a substantial local retention of larvae in proximity to the release areas, whereas the S_{sup} scenario shows extensive larval dispersal, as expected, particularly in the Gulf of Lion and the Strait of Sicily. These differences may be ascribed to the much stronger currents on the sea surface than at depth in the water column; the dispersion pattern in the S_{sup} scenario is therefore wider than in the S_{unif} scenario. The case of the Strait of Sicily represents a good example of this difference between the two scenarios (Fig. 4). Here dispersal occurs over a larger area in the S_{sup} scenario, likely due to the strong currents in this part of the Mediterranean Sea. However, even with wide dispersal, there is some agreement between results from the two scenarios, mainly for the Ionian Sea and Sardinian Channel. We acknowledge that the lack of information on *I. elongata* larval behaviour represents a limitation for this type of study (Leis, 2021), as highlighted in similar studies on deep-sea corals (Sciascia *et al.*, 2022).

Our results for the uniform release scenario agree with previous findings on *I. elongata*, in particular the limited dispersal ability (Otero *et al.*, 2017); the same has been observed in other gorgonian species such as *Paramunicea clavata*, for which population genetics indicates that short-distance dispersal is the most frequent (Coelho *et al.*, 2023). Knowledge of the larval behaviour of coral species is still incomplete because most species live at great depths, where it is quite difficult to collect data. Other studies have attempted to investigate the behaviour of larvae and the duration of the larval phase in other corals (Kenchington *et al.*, 2019; Sciascia *et al.*, 2022; Wang *et al.*, 2022); the few available reports indicate a pelagic larval stage lasting 7 to 90 days (Hilário *et al.*, 2015). Various studies based on population genetics, experimentation and in situ surveys suggest that larval retention in Mediterranean octocorals is high. With respect to other well-studied coral species such as *Corallium rubrum*, which is found at depths of 5-800 m and has a limited dispersal range (22.6-32.1 cm; Ledoux *et al.*, 2010a), there is very little information on the larval behaviour and dispersal of *I. elongata.* Experiments conducted on the gorgonian *P. clavata* indicate that the planulae of this species are able to postpone metamorphosis for a few days, suggesting a high dispersal potential (also

considering that this species is found in areas with rather high water velocities); however, in the case of *P. clavata*, larval sinking and adhesion to the substratum occurs near maternal colonies (Coma *et al.*, 1995; Linares *et al.*, 2008; Mokhtar Jamai *et al.*, 2013). This mechanism is different for other corals species, and dispersal distances vary from tens to hundreds of km (see Linares *et al.*, 2008 and references therein).

Results for the S_{sup} scenario suggest that larvae are less likely to reach the surface and be carried by surface currents across the Mediterranean. Nevertheless, outputs for this scenario suggest that hotspots for the arrival of *Isidella elongata* larvae are present in the Ionian Sea and the Sardinian Channel; these results are similar to those of the S_{unif} scenario. As the larval behaviour of corals can differ widely (Mulla *et al.*, 2020), future research should focus on this aspect. Larval position in the water column is important for the dispersal of many benthic species taxa, and traits regulating the vertical position of benthic species affect their dispersal (Queiroga *et al.*, 2007). Future studies should focus on investigating the connectivity of deep-water corals through combined molecular analysis and modelling: for example, dispersion models and habitat suitability modelling are widely used to understand relationships between species distribution and environmental conditions.

Our findings on genetic clustering and dispersal patterns suggest that there is *Isidella elongata* connectivity across the Mediterranean Sea. This is further confirmed by the haplotypes found in all samples (Fig. 3), although some differences emerged in the Aegean Sea, the Ionian Sea and the Ligurian Sea. The apparent difference between genetic results and the output of the Lagrangian model may reflect differences in the spatial and temporal resolution of the two adopted methods: genetic markers capture the gene flow over multiple generations, whereas Lagrangian simulations estimate present-day potential connectivity based on sea currents. The limited observed dispersal pattern (already proposed for *I. elongata*; Otero *et al.*, 2017) can probably be ascribed to the fact that *I. elongata* connectivity likely occurs through "stepping stones", which means that genetic information has been flowing across different areas of the Mediterranean through patches where the species is present. However, due to the severe impact of bottom trawling and habitat degradation (Otero *et al.*, 2017), many of these "intermediate" populations may have been extirpated in the last decades. As a result, only a few populations remain: while these are still genetically similar due to past connectivity, considering the resolution of the genetic markers used in this study (see Fig. 3), early signals of genetic differentiation are beginning to appear. The observed pattern may reflect an ongoing divergence process shaped by reduced gene flow, enhanced genetic drift and inbreeding. Long-term genetic monitoring, along with demographic modelling, will be essential in assessing its progression and in evaluating appropriate conservation efforts to be implemented.

Implications for biodiversity conservation

One of the objectives of EU policies (European Commission, 2023) is the conservation of Vulnerable Marine Ecosystems (VMEs) while improving the environmental sustainability of deep-sea fisheries. The protection of VMEs calls for the designation of a network of Fisheries Restricted Areas (FRAs) where all fishing activities (including longlines) are prohibited. To achieve full protection it is therefore necessary to both identify the location of species hotspots and acquire knowledge of connectivity corridors. This combined approach based on molecular and modelling techniques could be an innovative tool for identifying suitable areas for the conservation of the deep-sea habitats.

Some examples of a network of FRAs for the protection of VMEs are found in the northeast Atlantic, where several VME habitats have been mapped (ICES, 2020), although these are only based on species distribution models; the Mediterranean is lagging behind, with only four FRAs designated for the protection of different VMEs across the whole basin. The results of the present study can be used to inform decision-making processes pertaining to the identification of a Mediterranean network of areas for the protection of the VME identified by the presence of *Isidella elongata*. In particular, identified dispersal patterns can be used as a basis for further investigation and for future fishery management plans to mitigate the impact of bottom trawlers on VMEs. In this context, it should be noted that, based on the historical development of trawling for deep-water red shrimp (DWRS), Fiorentino *et al.* (2024) proposed a management approach for deep-water bottom trawling where, together with the adoption of a catch control regime, fishing is only allowed in selected areas with low presence of critical habitats and high DWRS catch rates. Our results support the ongoing mapping of the habitat suitability of VME indicator species affected by climate and fishery impacts at the Mediterranean scale (Georges *et al.*, 2024; Millot *et al.*, 2024). Given that rapid intervention is required to protect endangered species, it is important to understand all ecological aspects that influence and explain their spatial patterns. This is because several processes affect population connectivity (e.g., larval behaviour, availability of suitable habitat, biotic interactions and fishing pressure), resulting in complex, varied connectivity patterns. From a conservation standpoint, it is important to identify areas that support vulnerable habitats while considering socio-economic limitations.

Acknowledgements

We would like to thank all the people that helped to collect the samples to perform the genetic analysis. We thank Lorenzo Bramanti for his suggestions and insights when the work was conceived.

Declaration of interests: The authors declare that they have no known competing financial interests or per-

sonal relationships that could have appeared to influence the work reported in this paper. **Authors contribution:** VL, GG, LV, FF, MA: designed research VL. FG, LV , OC, JFF: performed research and analysed data**.** All authors: wrote the paper. **Funding:** Project funded under the National Recovery and Resilience Plan (NRRP), Mission 4 Component 2 Investment 1.4 - Call for tender No. 3138 of 16 December 2021, rectified by Decree n.3175 of 18 December 2021 of Italian Ministry of University and Research funded by the European Union - NextGenerationEU, project code CN_00000033, Concession Decree No. 1034 of 17 June 2022 adopted by the Italian Ministry of University and Research, CUP D33C22000960007, project title "National Biodiversity Future Center - NBFC"; and by "Crédit de Recherches" grant J.0077.25 (projet "CoGeS") of the F.R.S.-FNRS to JFF.

References

Angiolillo, M., Di Lorenzo, B., Izzi, A., Giusti, M., Nonnis, O. *et al.* 2024. Healthy assemblages of *Isidella elongata* unintentionally protected from trawling offshore of Asinara Island (northwestern Sardinia, NW Mediterranean Sea). *Scientific Reports*, 14 (1), 12813.

Aurelle, D., Pivotto, I.D., Malfant, M., Topçu, N.E., Masmoudi, M.B. *et al.*, 2017. Fuzzy species limits in Mediterranean gorgonians (Cnidaria, Octocorallia): Inferences on speciation processes. *Zoologica Scripta*, 46 (6), 767-778.

Bandelt, H.J., Forster, P., Röhl, A., 1999. Median-joining networks for inferring intraspecific phylogenies. *Molecular Biology and Evolution*, 16 (1), 37-48.

Bayer, F., Stefani, J., 1987. *Isididae (Gorgonacea) de Nouvelle-Calédonie. Nouvelle clé des genres de la famille. Bulletin du Mus é um National d'Histoire Naturelle de Paris,* 4 (9), 47-106.

Bongiorni, L., Mea, M., Gambia, C., Pusceddu, A., Taviani, M. *et al.* 2010. Deep-water scleractinian corals promote higher biodiversity in deep-sea meiofaunal assemblages along continental margins. *Biological Consrvation*, 143 (7), 1687-1700.

Brugler, M.R., France, S.C., 2008. The mitochondrial genome of a deep-sea bamboo coral (Cnidaria, Anthozoa, Octocorallia, Isididae): genome structure and putative origins of replication are not conserved among octocorals. *Journal of Molecular Evolution*, 67 (2), 125-136.

Buhl-Mortensen, L., Vanreusel, A., Gooday, A.J., Levin, L.A., Priede, I.G. *et al.*, 2010. Biological structures as a source of habitat heterogeneity and biodiversity on the deep ocean margins. *Marine Ecology*, 31 (1), 21-50.

Calderón, I., Garrabou, J., Aurelle, D., 2006. Evaluation of the utility of COI and ITS markers as tools for population genetic studies of temperate gorgonians. *Journal of Experimental Marine Biology and Ecology*, 336 (2), 184-197.

Carbonara, P., Zupa, W., Follesa, M. C., Cau, A., Capezzuto, F. *et al.*, 2020. Exploring a deep-sea vulnerable marine ecosystem: *Isidella elongata* (Esper, 1788) species assemblages in the Western and Central Mediterranean. *Deep Sea Research Part I: Oceanographic Research Papers*, 166, 103406.

Carbonara, P., Zupa, W., Follesa, M.C., Cau, A., Donnaloia, M. *et al.*, 2022. Spatio-temporal distribution of *Isidella elongata*, a vulnerable marine ecosystem indicator species, in the southern Adriatic Sea. *Hydrobiologia*, 849 (21), 4837-4855.

Carpine, C., Grasshoff, M., 1975. *Les gorgonaires de la Méditerranée occidentale. Bulletin de l'Institut Océanographique de Monaco*, 71 (1430), 140 p

Cartes, J.E., Díaz-Viñolas, D., González-Irusta, J.M., Serrano, A., Mohamed, S. *et al.*, 2022. The macrofauna associated to the bamboo coral *Isidella elongata*: To what extent the impact on isideidae affects diversification of deep-sea fauna. *Coral Reefs*, 41 (4), 1273-1284.

CBD/COP/15/L.25 Kunming-Montreal Global biodiversity framework, 18 Dec. 2022,

Chimienti, G., Bo, M., Taviani, M., Mastrototaro, F., 2019. 19 occurrence and biogeography of *Mediterranean cold-water corals. In: Mediterranean Cold-Water Corals: Past, Present and Future*, C. Orejas, C. Jiménez (Eds.) Understanding the Deep-Sea Realms of Coral (pp. 213-243). Cham: Springer International Publishing.

Chimienti, G., Mastrototaro, F., D'Onghia, G., 2020. Mesophotic and deep-sea vulnerable coral habitats of the Mediterranean sea: overview and conservation perspectives. In L. A. Soto (Ed.), *Advances in the Studies of the Benthic Zone*. IntechOpen.

Coelho, M.A.G., Pearson, G.A., Boavida, J.R.H., Paulo, D., Aurelle, D. *et al.*, 2023. Not out of the Mediterranean: Atlantic populations of the gorgonian *Paramuricea clavata* are a separate sister species under further lineage diversification. *Ecology and Evolution*, 13 (1), e9740.

Coll, M., Piroddi, C., Steenbeek, J., Kaschner, K., Ben Rais Lasram, F. *et al.*, 2010. The biodiversity of the Mediterranean sea: estimates, patterns, and threats. *PLoS ONE*, 5 (8), e11842.

Coma, R., Ribes, M., Zabala, M., Giti, J., 1995. Reproduction and cycle of gonadal development in the Mediterranean gorgonian *Paramuricea clavata*. *Marine Ecology Progresses Series,* 117, 173-183.

Danovaro, R., Pusceddu, A., 2007.Ecomanagement of biodiversity and ecosystem functioning in the Mediterranean Sea: concerns and strategies. *Chemistry and Ecology* 23, 347-360.

Doyle, J.J., 1995. The irrelevance of allele tree topologies for species delimitation, and a non-topological alternative. *Systematic Botany*, 20 (4), 574-588.

European Commission, 2023. *Improving environmental sustainability of deep sea fisheries with emphasis on the conservation of Vulnerable Marine Ecosystems (VMEs): Final report.* Publications Office.

Fabri, M.C., Pedel, L., Beuck, L., Galgani, F., Hebbeln, D. *et al.,* 2014. Megafauna of vulnerable marine ecosystems in French mediterranean submarine canyons: Spatial distribution and anthropogenic impacts. *Deep-Sea Research Part II: Topical Studies in Oceanography*, 104, 184-207.

Fiorentino, F., Garofalo, G., Bono, G.,Vitale, S., 2024. Learning from the history of red shrimp fisheries in the Mediterranean to improve sustainability of deep-water bottom trawling. *ICES Journal of Marine Science*, 81 (4), 652-664.

Flot, J.F., 2007. Champuru 1.0: A computer software for unraveling mixtures of two DNA sequences of unequal lengths. *Molecular Ecology Notes*, 7 (6), 974-977.

Flot, J.F., Couloux, A., Tillier, S., 2010. Haplowebs as a graphical tool for delimiting species: a revival of Doyle's "field for recombination" approach and its application to the coral genus *Pocillopora* in Clipperton. *BMC Evolutionary Biology*, 10, 372.

Flot, J.F., 2010. SeqPHASE: A web tool for interconverting phase input/output files and fasta sequence alignments. *Molecular Ecology Resources*, 10 (1), 162-166.

Flot, J.F., Magalon, H., Cruaud, C., Couloux, A., Tillier, S., 2008. Patterns of genetic structure among Hawaiian corals of the genus *Pocillopora* yield clusters of individuals that are compatible with morphology. *Comptes Rendus Biologies*, 331 (3), 239-247.

Flot, J.F., Tillier, S., 2006. Molecular phylogeny and systematics of the scleractinian coral genus *Pocillopora* in Hawaii. Proceedings of the 10th International Coral Reef Symposium, 1, 24-29.

Folmer, O., Black, M., Hoeh, W., Lutz, R., Vrijenhoek, R., 1994. DNA primers for amplification of mitochondrial cytochrome *c* oxidase subunit I from diverse metazoan invertebrates. *Molecular Marine Biology and Biotechnology*, 3 (5), 294-299.

Fontaneto, D., Flot, J.F., Tang, C. Q., 2015. Guidelines for DNA taxonomy, with a focus on the meiofauna. *Marine Biodiversity*, 45 (3), 433-451.

Gargano, F., Garofalo, G., Fiorentino, F., 2017. Exploring connectivity between spawning and nursery areas of *Mullus barbatus* (L., 1758) in the Mediterranean through a dispersal model. *Fisheries Oceanography*, 26 (4), 476-497.

Gargano, F., Garofalo, G., Quattrocchi, F., Fiorentino, F., 2022. Where do recruits come from? Backward Lagrangian simulation for the deep water rose shrimps in the Central Mediterranean Sea. *Fisheries Oceanography*, 31 (4), 369-383.

Georges, V., Vaz, S., Carbonara, P., Fabri, M.C., Fanelli, E. *et al.,* 2024. Mapping the habitat refugia of *Isidella elongata* under climate change and trawling impacts to preserve Vulnerable Marine Ecosystems in the Mediterranean. *Scientific Reports*, 14 (1), 6246.

Gerovasileiou, V., Smith, C. J., Kiparissis, S., Stamouli, C., Dounas, C. *et al.*, 2019. Updating the distribution status of the critically endangered bamboo coral *Isidella elongata* (Esper, 1788) in the deep Eastern Mediterranean Sea. *Regional Studies in Marine Science*, 28, 100610.

Getis, A., Ord, J.K., 1992. The analysis of spatial association by use of distance statistics. *Geographical Analysis*, 24 (3), 189-206.

González-Irusta, J.M., Cartes, J.E., Punzón, A., Díaz, D., de Sola, L.G. *et al.*, 2022. Mapping habitat loss in the deep-sea using current and past presences of *Isidella elongata* (Cnidaria: Alcyonacea). *ICES Journal of Marine Science*, 79 (6), 1888-1901.

Gori, A., Bramanti, L., López-González, P., Thoma, J.N., Gili, J.M. *et al.*, 2012. Characterization of the zooxanthellate and azooxanthellate morphotypes of the Mediterranean gorgonian *Eunicella singularis* . *Marine Biology*, 159, 1485-1496.

Grilli, F., Pinardi, N., 1998. The computation of Rossby radii of deformation for the Mediterranean Sea. *MTP News*, 4-5.

Guindon, S., Dufayard, J.-F., Lefort, V., Anisimova, M., Hordijk, W. *et al.*, 2010. New algorithms and methods to estimate maximum-likelihood phylogenies: assessing the performance PhyML 3.0. *Systematic Biology*, 59 (3), 307321.

Guizien, K., Bramanti, L., 2014. Modelling ecological complexity for marine species conservation: The effect of variable connectivity on species spatial distribution and age-structure. *Theoretical Biology Forum*, 107, 47-56.

Hebert, P.D.N., Cywinska, A., Ball, S. L., deWaard, J.R., 2003. Biological identifications through DNA barcodes. *Proceedings of the Royal Society of London. Series B: Biological Sciences*, 270 (1512), 313–321.

Hellberg, M.E., Burton, R.S., Neigel, J.E., Palumbi, S.R., 2002. Genetic assessment of connectivity among marine populations. *Bulletin of Marine Science*, 70 (1), 273-290.

Hilário, A., Metaxas, A., Gaudron, S.M., Howell, K.L., Mercier, A. *et al.*, 2015. Estimating dispersal distance in the deep sea: Challenges and applications to marine reserves. *Frontiers in Marine Science*, 2, 6.

Huang, D., Meier, R., Todd, P.A., Chou, L.M., 2008. Slow mitochondrial COI sequence evolution at the base of the metazoan tree and its implications for DNA Barcoding. *Journal of Molecular Evolution*, 66 (2), 167-174.

Huret, M., Runge, J., Chen, C., Cowles, G., Xu, Q., *et al.* 2007. Dispersal modeling of fish early life stages: Sensitivity with application to Atlantic cod in the western Gulf of Maine. *Marine Ecology Progress Series*, 347, 261-274..

ICES, 2020. *Workshop on EU regulatory area options for VME protection*.

Katoh, K., Rozewicki, J., Yamada, K.D., 2019. MAFFT online service: Multiple sequence alignment, interactive sequence choice and visualization. *Briefings in Bioinformatics*, 20 (4), 1160-1166.

Kenchington, E., Wang, Z., Lirette, C., Murillo, F.J., Guijarro, J. *et al.*, 2019. Connectivity modelling of areas closed to protect vulnerable marine ecosystems in the northwest Atlantic. *Deep Sea Research Part I: Oceanographic Research Papers*, 143, 85-103.

Korfhage, S.A., Rossel, S., Brix, S., McFadden, C.S., Ólafsdóttir, S.H. *et al.*, 2022. Species delimitation of Hexacorallia and Octocorallia around Iceland using nuclear and mitochondrial DNA and proteome fingerprinting. *Frontiers in Marine Science*, 9, 838201.

Lacorata, G., Mazzino, A., Rizza, U., 2008. 3D chaotic model for sub-grid turbulent dispersion in large eddy simulations. *Journal of the Atmospheric Sciences*, 65 (7), 2389-2401.

Lacorata, G., Palatella, L., Santoleri, R., 2014. Lagrangian predictability characteristics of an Ocean Model. *Journal of Geophysical Research: Oceans*, 119 (11), 8029-038.

Laubier, L., Emig, C.C., 1993. La faune benthique profonde de Méditerranée, 397-428.

Lauria, V., Garofalo, G., Fiorentino, F., Massi, D., Milisenda, G. *et al.*, 2017. Species distribution models of two critically endangered deep-sea octocorals reveal fishing impacts on vulnerable marine ecosystems in central Mediterranean Sea. *Scientific Reports*, 7 (1), 1-14.

Ledoux, J.B., Mokhtar-Jamaï, K., Roby, C., Féral, J.P., Garrabou, J. *et al.*, 2010a. Genetic survey of shallow populations of the Mediterranean red coral [*Corallium rubrum* (Linnaeus, 1758)]: new insights into evolutionary processes shaping nuclear diversity and implications for conservation. *Molecular Ecology*, 19 (4), 675-90.

Ledoux, J.B., Garrabou, J., Bianchimani, O., Drap, P., Féral,

J.P. *et al.*, 2010b. Fine-scale genetic structure and inferences on population biology in the threatened Mediterranean red coral, *Corallium rubrum. Molecular Ecology*, (19), 4204-4216.

Le Goff-Vitry, M.C., Pybus, O. G., Rogers, A.D., 2004. Genetic structure of the deep-sea coral *Lophelia pertusa* in the northeast Atlantic revealed by microsatellites and internal transcribed spacer sequences. *Molecular Ecology*, 13 (3), 537-549.

Lejeusne, C., Chevaldonné, P., Pergent-Martini, C., Boudouresque, C.F., Pérez, T., 2010. Climate change effects on a miniature ocean: The highly diverse, highly impacted Mediterranean Sea. *Trends in Ecology & Evolution*, 25 (4), 250-260.

Leis, J.M., 2021. Perspectives on larval behaviour in biophysical modelling of larval 588 dispersal in marine, demersal fishes. *Oceans*, 2 (1),1 -25.

Liao, D., 1999. Concerted evolution: molecular mechanism and biological implications. *American Journal of Human Genetics*, 64, 24-30.

Linares, C., Coma, R., Mariani, S., Díaz, D., Hereu, B. *et al.,* 2008. Early life history of the Mediterranean gorgonian *Paramuricea clavata*: implications for population dynamics. *Invertebrate Biology,* 127, 1-11.

Mackenzie, C.L., Kent, F.E.A., Baxter, J.M., Gormley, K.S.G., Cassidy, A.J. *et al*., 2022. Genetic connectivity and diversity of a protected, habitat-forming species: evidence demonstrating the need for wider environmental protection and integration of the marine protected area network. *Frontiers in Marine Science*, 9, 772259.

Martínez-Quintana, A., Bramanti, L., Viladrich, N., Rossi, S., Guizien, K., 2015. Quantification of larval traits driving connectivity: The case of *Corallium rubrum* (L. 1758). *Marine Biology*, 162 (2), 309-318.

Mastrototaro, F., Chimienti, G., Acosta, J., Blanco, J., Garcia, S. *et al.*, 2017. *Isidella elongata* (Cnidaria: Alcyonacea) facies in the western Mediterranean Sea: Visual surveys and descriptions of its ecological role. *The European Zoological Journal*, 84 (1), 209-225.

Maynou, F., Cartes, J.E., 2012. Effects of trawling on fish and invertebrates from deep-sea coral facies of *Isidella elongata* in the western Mediterranean. *Journal of the Marine Biological Association of the United Kingdom*, 92, 1501-1507.

Metaxas, A., Lacharité, M., de Mendonça, S.N., 2019. Hydrodynamic connectivity of habitats of deep-water corals in Corsair Canyon, northwest Atlantic: a case for cross-boundary conservation. *Frontiers in Marine Science*, 6, 159.

Millot, J., Georges, V., Lauria, V., Hattab, T., Dominguez-Carrió, C. *et al.* 2024. Habitat shifts of the vulnerable crinoid *Leptometra phalangium* under climate change scenarios. *Progress in Oceanography*, 229, 103355.

Mokthar-Jamai, K., Pascual, M., Ledoux, J.B., Coma, R., Féral, J.P. *et al.*, 2011. From global to local genetic structuring in the red gorgonian *Paramuricea clavata*: the interplay between oceanographic conditions and limited larval dispersal. *Molecular Ecology,* 20, 3291-3305.

Mokhtar-Jamai, K., Coma, R., Wang, J., Zuberer F., Féral, J.P. *et al.*, 2013. Role of evolutionary and ecological factors in the reproductive success and the spatial genetic structure of the temperate gorgonian *Paramuricea clavata*. *Ecology and Evolution,* 3 (6), 1765-1779.

Mulla, A.J., Lin, C.-H., Takahashi, S., Nozawa, Y., 2020. Species-specific phototaxis of coral larvae causes variation in vertical positioning during dispersal. *bioRxiv*, 2020.07.31.230235.

Mytilineou, C., Smith, C.J., Anastasopoulou, A., Papadopoulou, K.N., Christidis, G., 2014. New cold-water coral occurrences in the Eastern Ionian Sea: Results from experimental long line fishing. *Deep-Sea Research Part I: Oceanographic Research Papers*, 99, 146-157.

Otero, M.M., Numa, M., Orejas, C., Garrabou, J., Cerrano, C. *et al.*, 2017. *Overview of the conservation status of Mediterranean anthozoans.* IUCN International Union for Conservation of Nature.

Palatella, L., Bignami, F., Falcini, F., Lacorata, G., Lanotte, A.S. *et al.*, 2014. Lagrangian simulations and interannual variability of anchovy egg and larva dispersal in the Sicily Channel. *Journal of Geophysical Research: Oceans*, 119 (2), 1306-1323.

Pineda, J., Hare, J.A., Sponaugle, S., 2007. Larval transport and dispersal in the coastal ocean and consequences for population connectivity. *Oceanography*, 20, 22-39.

Pont-Kingdon, G.A., Okada, N.A., Macfarlane, J.L., Beagley, C.T., Wolstenholme, D.R. *et al.*, 1995. A coral mitochondrial *mutS* gene. *Nature*, 375 (6527), 109-111.

Quattrocchi, G., Sinerchia, M., Colloca, F., Fiorentino, F., Garofalo, G. *et al.*, 2019. Hydrodynamic controls on connectivity of the high commercial value shrimp *Parapenaeus longirostris* (Lucas, 1846) in the Mediterranean Sea. *Scientific Reports*, 9 (1), 16935.

Queiroga, H., Cruz, T., Santos, A. dos, Dubert, J., González-Gordillo, *et al.*, 2007. Oceanographic and behavioural processes affecting invertebrate larval dispersal and supply in the western Iberia upwelling ecosystem. *Progress in Oceanography*, 74 (2), 174-191.

Ronquist, F., Teslenko, M., van der Mark, P., Ayres, D.L., Darling, A. *et al.*, 2012. MrBayes 3.2: Efficient bayesian phylogenetic inference and model choice across a large model space. *Systematic Biology*, 61 (3), 539-542.

Rossi, L., 1971. *Cnidari e ctenofori d'Italia* (2; pp. 77–92). Quaderni della Civica Stazione Idrobiologica di Milano.

Rueda, J. L., Urra, J., Aguilar, R., Angeletti, L., Bo, M. *et al.*, 2019. Cold-Water Coral Associated Fauna in the Mediterranean Sea and Adjacent Areas. In C. Orejas, C. Jiménez (Eds.), *Mediterranean Cold-Water Corals: Past, Present and Future.* Springer International Publishing.

Sánchez, J.A., McFadden, C.S., France, S.C., Lasker, H.R., 2003. Molecular phylogenetic analyses of shallow-water Caribbean octocorals. *Marine Biology*, 142 (5), 975-987.

Saucier, E.H., 2016. *Phylogenetic studies of the deep-sea bamboo corals (Octocorallia: Isididae: Keratoisidinae)*. Doctor of Philosophy Dissertation]. Graduate Faculty of the University of Louisiana at Lafayette.

Sciascia, R., Guizien, K., Magaldi, M.G., 2022. Larval dispersal simulations and connectivity predictions for Mediterranean gorgonian species: Sensitivity to flow representation and biological traits. *ICES Journal of Marine Science*, 79 (7), 2043-2054.

Shearer, T.L., van Oppen, M.J.H., Romano, S.L., Wörheide, G., 2002. Slow mitochondrial DNA sequence evolution

in the Anthozoa (Cnidaria). *Molecular Ecology*, 11(12), 2475-2487.

Spöri, Y., Flot, J.F., 2020. HaplowebMaker and CoMa: Two web tools to delimit species using haplowebs and conspecificity matrices. *Methods in Ecology and Evolution*, 11 (11), 1434-1438.

Spöri, Y., Flot, J.F., 2024. *Champuru 2: Improved scoring of alignments and a user-friendly graphical interface*. arXiv preprint arXiv:2405.06032.

Tamura, K., Stecher, G., Kumar, S., 2021. MEGA11: Molecular Evolutionary Genetics Analysis Version 11. *Molecular Biology and Evolution*, 38 (7), 3022-3027.

Terrana, L., Flot, J.F., Eeckhaut, I., 2021. ITS1 variation among *Stichopathes* cf. *maldivensis* (Hexacorallia: Antipatharia) whip black corals unveils conspecificity and population connectivity at local and global scales across the Indo-Pacific. *Coral Reefs*, 40 (2), 521-533.

Thompson, J. D., Higgins, D. G., Gibson, T. J., 1994. CLUSTAL W: improving the sensitivity of progressive multiple sequence alignment through sequence weighting, position-specific gap penalties and weight matrix choice. *Nucleic Acids Research*, 22 (22), 4673-4680.

Torri, M., Russo, S., Falcini, F., De Luca, B., Colella, S. *et al.*, 2023. Coupling Lagrangian simulation models and remote sensing to explore the environmental effect on larval growth rate: The Mediterranean case study of round sardinella (*Sardinella aurita*) early life stages. *Frontiers in Marine Science*, 9, 1065514.

Wang, S., Murillo, F.J., Kenchington, E., 2022. Climate-change refugia for the bubblegum coral *Paragorgia arborea* in the Northwest Atlantic. *Frontiers in Marine Science*, 9, 863693.

White, C., Selkoe, K.A., Watson, J., Siegel, D.A., Zacherl, D.C. *et al.*, 2010. Ocean currents help explain population genetic structure. *Proceedings of the Royal Society B: Biological Sciences*, 277 (1688), 1685-1694.

APPENDIX

The lagrangian model

The first velocity field $U_{2D}= (u_{2D} , v_{2D})$ is obtained from the stream function

$$\Psi = \frac{A}{k}\sin[k(x - \varepsilon\sin(\omega t)]\sin[k(y - \varepsilon\cos(\omega t)]$$

i.e. $\partial_x\Psi = v_{2D}$ and $\partial_y\Psi = -u_{2D}$, where A = 0.1 m/s, $\varepsilon = 0.1I_0$, $\omega = 2\pi A_0/I_0$ and $k = 2\pi/I_0$; I_0 =20 km. The second superimposed velocity field is a 3D field $U_{3D} = (u_{3D} , v_{3D}, w_{3D})$, is obtained from the potential vector $\Phi = (\Phi_1, \Phi_2)$ as $\partial_z\Phi_1 = u_{3D}, \partial_z\Phi_2 = -v_{3D}, -\partial_x\Phi_1 + \partial_y\Phi_2 = w_{3D}$.

The components (Φ_1, Φ_2) are defined according to

$$\Phi_1 = \frac{A_1}{k_1}\sin[k_1(x - \varepsilon_1\sin(\omega_1 t)]\sin[k_1(z - \varepsilon_1\cos(\omega_1 t)],$$

$$\Phi_2 = \frac{A_2}{k_2}\sin[k_2(x - \varepsilon_2\sin(\omega_2 t)]\sin[k_2(z - \varepsilon_2\cos(\omega_2 t)],$$

where A_1 = 0.036 m/s, ε_1=0.2I_1 ω_1=2πA_1/I_1, k_1=2π/I_1, A_2 = 0.041 m/s, ε_2=0.2I_2 ε_2=0.2I_2, ω_2=2π A/I_2, k_2 = 2π/I_2 where I_1 = 30 m and I_2 = 42 m. Moreover, to address the absence of the "sweeping" effect due to the transport of small eddies trough the larger and more energetic eddies, see Thomson and Devenish (2005) and Lacorata et al. (2014), the quasi-Lagrangian approach was adopted. According to this approach, each pair of initially close particles moves in its own kinematic field anchored to its mass center, advected by the main current velocity field U_{MFS}, and the relative motion of the particles is governed by the velocity fields U_{2D} and U_{3D}. In particular, given $r_{1,2}(t) = (x_{1,2}(t), y_{1,2}(t), z_{1,2}(t))$ the position vectors (longitude, latitude and depth) of two initially close particles , $r_c(t) = (x_c(t), y_c(t), z_c(t))$ the mass center of the two particles and $\underline{r}_{1,2}(t) = (\underline{x}_{1,2}(t), \underline{y}_{1,2}(t), \underline{z}_{1,2}(t))$ the relative coordinates computed in frame of reference centered in $r_c(t)$, the time evolution of the pair is obtained by the system of equations

$$\begin{cases} \dfrac{dx}{dt} = u_{MFS}(x_c, t) + u_{2D}(\underline{x}, t) + u_{3D}(\underline{x}, t) \\ \dfrac{dy}{dt} = v_{MFS}(y_c, t) + v_{2D}(\underline{y}, t) + v_{3D}(\underline{y}, t) \\ \dfrac{dz}{dt} = w_{3D}(\underline{z}, t) \end{cases}$$

The numerical solutions of the Lagrangian system were derived using a fourth-order Runge-Kutta temporal scheme with a time step of 120 seconds. As the velocity field U_{MFS} is provided in specific cell positions, the exact value of U_{MFS} ($r_c(t)$)at $r_c(t)$ is obtained through horizontal bilinear interpolation on the nine grid cells surrounding. Since U_{MFS} exhibits temporal discontinuity when transitioning from one day to the next, U_{MFS} was linearly weighted between two consecutive days from 16:00 PM to 00:00 AM, ensuring that the velocity field of a specific day smoothly transitioned to that of the following day. Finally, reflective boundary conditions for the particles were imposed along the basin boundaries.